Geology, petrography and geochemistry of the acid volcanism of the Paraná Magmatic Province in the Piraju-Ourinhos region, SE Brazil

Valdecir de Assis Janasi[1], Tarcísio José Montanheiro[2], Vivian Azor de Freitas[1], Pedro Morais Reis[1], Francisco de Assis Negri[2] & Fernanda Amaral Dantas[1]

Abstract A succession of trachydacitic lava flows over 150 m thick constitutes the lowermost portion of the Serra Geral Fm. along the Paranapanema River valley in the Piraju-Ourinhos region, State of São Paulo. The flows have a well-defined zonality: the central portion is made up of grey porphyritic dacites with low glass and vesicle proportion which grade towards the contacts to strongly vesiculated varieties with glassy groundmass which, when in contact with the Botucatu Fm. basal sandstones or with larger bodies of inter-flow sandstone, show a typical chocolate-brown color. The observed compositional variation is small, and in part a reflection of secondary alteration. Independent of texture, mode of occurrence and stratigraphic position, the rocks show similar contents of SiO_2 (65-67 wt%) and all other major oxides, and a ferrous (mg#= 20-27) and metaluminous A/CNK= 0.85-0.95) character; alteration associated to vesicle infilling and color change to chocolate-brown results in lower mg# and higher A/CNK. Mineral and whole rock chemical data indicate high crystallization temperatures around 1000ºC (pyroxene thermometry; apatite saturation), consistent with the predominant mode of occurrence as flows.

Keywords: trachydacite, Serra Geral Fm., Paraná Magmatic Province, mineral chemistry, magma temperatures.

Resumo *Geologia, petrografia e geoquímica do vulcanismo ácido da Província Magmática Paraná, na região de Piraju-Ourinhos, SE Brasil.* Uma sucessão de derrames de composição traquidacítica com espessura superior a 150 m constitui a base da Fm. Serra Geral em uma faixa de ca. 60 km ao longo da calha do rio Paranapanema, entre as cidades de Piraju e Ourinhos (SP). Os derrames mostram zonalidade bem marcada: a porção central é formada por dacitos porfiríticos cinza com baixa proporção de vidro e vesículas, que gradam, em direção aos contatos, para variedades vítreas fortemente vesiculadas que, em contato com arenitos basais da Fm. Botucatu ou com corpos maiores de arenitos inter-derrame, apresentam cor marrom-chocolate característica. A variação composicional observada é muito pequena, e em parte devida a efeitos secundários. De modo independente das texturas, forma de ocorrência e posição estratigráfica, as rochas apresentam teores similares de SiO_2 (65-67%) e todos os demais óxidos maiores, caráter ferroso (mg#= 20-27) e metaluminoso (A/CNK= 0,85-0,95); a alteração associada ao preenchimento de vesículas e geração da cor chocolate se reflete na diminuição de mg# e aumento de A/CNK. Dados de química de minerais e de rocha indicam temperaturas liquidus elevadas, próximas a 1000ºC (termometria de piroxênios; saturação em apatita), consistente com modo de ocorrência predominante na forma de derrames.

Palavras-Chave: dacito, Fm. Serra Geral, Província Magmática Paraná, química mineral, temperaturas de magmas.

INTRODUCTION Acid volcanic rocks, which comprise ca. 2.5% of the volume in the cretaceous Paraná-Etendeka Magmatic Province (PEMP), are distributed very assymetrically: they are absent in the NNW portion of the Paraná Basin, where the earliest basaltic flows appear (Stewart *et al.*, 1996), and are very expressive in the SSE portion (and the African counterpart in the Etendeka region), where they were emplaced typically in the upper portion of the lava pile (e.g., Bellieni *et al*. 1986; Garland *et al.* 1995).

The acid volcanic rocks of the Piraju-Ourinhos region outcrop in a ca. 60 km long area parallel to the Paranapanema River in the border between the Paraná and São Paulo States, and are the northernmost in the Paraná Basin, constituting locally the basis of the volcanic pile, directly in contact with the aeolic sediments of the Botucatu Fm. (Raposo 1987; Iyomasa *et al.* 1994). Previous works in this region focused on the lithogeochemistry of these rocks and associated basalts (Raposo 1987) and their mineralogical and textural characteristics, with emphasis on their potential use as pozzolanic material (Montanheiro 1999).

In this work, we present the initial results of a research project that investigates the geology and petrology of the acid volcanism in Piraju-Ourinhos. Semi-detailed geological mapping and the intergration

1 - Instituto de Geociências, USP, São Paulo (SP), Brasil. E-mail: vajanasi@usp.br
2 - Instituto Geológico, Secretaria do Meio Ambiente do Estado de São Paulo, São Paulo (SP), Brasil.
E-mail: tjmonta@igeologico.sp.gov.br

of previous maps allowed evaluate more precisely the extension of occurrence of the acid volcanic roks; individualization in map of the different igneous bodies (flows, vents, dikes) is in progress. We obtained new chemical data for whole rock and minerals, which bring important constraints to the petrogenesis of the acid volcanism in the region. New geochemical data for the associated basalts are presented in another publication (Janasi *et al.* 2007).

THE ACID MAGMATISM IN THE PARANÁ MAGMATIC PROVINCE

General aspects The PEMP (ca. 138-127 Ma) represents one of the largest continental volcanic events of Planet Earth, extending for about 1,200,000 km^2 in central-south Brazil and neighboring countries (Paraguay, Argentina and Uruguay); the occurrences in Etendeka, Namibia, represent the continuity of the province in the African continent. The lava volume is estimated at ca. 800,000 km^3, with maximum thicknesses reaching locally 1,700 m at the central axis of the Paraná Basin. Tholeiitic basalts are largely predominant (>70% in volume), and were initially divided in two subtypes: those with high TiO_2, predominant in the northern portion of the Paraná Basin, and those with low (<2%) TiO_2, in the south (e.g., Bellieni *et al.* 1984; Peate 1997). More detailed geochemical and isotopic studies, including continuous stratigraphic sections studied in the field or obtained from sampling of deep boreholes allowed a more detailed basalt typology to be defined, and seven main types were distinguished, four with high Ti/Y and three with low Ti/Y (Peate 1997). Intermediate and acid volcanic rocks are more common in the SE portion of the Paraná Basin, where a variety described as Palmas type, having important chemical affinities with the low Ti/Y basalts, is predominant. Volumetrically less expressive occurrences in the center-north portion of the Paraná Basin (States of Paraná and São Paulo) are recognized as a second type (Chapecó), which shows geochemical and isotopic affinities with the high Ti/Y basalts.

Precise estimates of the age of the volcanism were only possible with the advent of Ar-Ar ages during the 1990 decade, and suggest an age migration from NNW (138-135 Ma) to SE (131-127 Ma); the main volume of magmas was generated in a small time interval (ca. 5 Myr., from 135 to 131 Ma; Stewart *et al.* 1996), during which some northward migration of the magmatism seems to have occurred locally (Ernesto *et al.* 1999).

Typology of the acid magmatism In the southern portion of the Paraná Basin, the acid volcanic rocks are more abundant, and occur typically at the top of the volcanic pile. Low Ti (plus P and other incompatible elements) rhyolites and rhyodacites are predominant, show a wide range of silica contents (64 to 72 wt%), and are grouped into the "Palmas type". Geochemical and isotopic evidence indicate that these acid rocks were produced by crystal fractionation of low-Ti basalts (Gramado type) associated to assimilation of high Rb/Ba partial melts produced by melting of intermediate to upper crust (Bellieni *et al.* 1986; Garland *et al.* 1995).

The second group of acid volcanic rocks, predominant in the central-northern portion of the Paraná Basin, and known as "Chapecó type", is represented by dacites, rhyodacites, quartz latites and rhyolites. These rocks have higher Ti (plus P and HFSE) contents, and are on average silica-poorer (64 to 68 wt% SiO_2), if compared to the Palmas type. They are characteristically porphyritic, with up to 25 vol.% phenocrysts. Petrographic, geochemical and isotopic evidence suggest an origin by remelting of high-Ti basalt underplates (Bellieni *et al.* 1986; Garland *et al.* 1995), although some authors consider that they could be products of anatexis of pre-existing crust (Harris & Milner 1997). Contrarily to observed in the Palmas type, plagioclase and pyroxene phenocrysts show no signs of resorption and have compositions compatible with that of the coexisting liquid (Garland *et al.* 1995). The relatively low contents of normative quartz are consistent with the granite eutectic at high pressure (between 5 and 15 kbar; Garland *et al.* 1995). Pyroclastic textures are rare, and it is suggested that magma ascension was fast, probably in dykes; in fact, the few dykes of acid composition known in the Paraná-Etendeka Magmatic Province (PEMP) are chemically equivalent to the Chapecó type (Garland *et al.* 1995).

LOCAL GEOLOGY Figure 1 is a preliminary geological map of Piraju-Ourinhos region (SP-PR), resulting from geological mapping in a semi-detail scale (1:100,000) and the integration of previously presented regional maps (CPRM unpublished data; Raposo 1987; Iyomasa et al. 1994).

The acid volcanic rocks occupy an area of *ca.* 65 x 20 km along N40W, following the direction of the Paranapanema River. The outcrop area is larger than shown in previous maps, since they extend much to the south of the Paranapanema River, forming the elevated plateau known locally as Fartura Hill. Apparently, the lack of sufficient petrographic support and/or scarcity of outcrops have contributed to the non identification of these rocks in the plateau in previous works. Their area of occurrence must be responsible for the local inflection of the "Serra Geral plateau", from its regional NNE direction to N40W, as a response to the greater resistance to erosion of these rocks, if compared to the basalts.

As observed in previous works in the area (Raposo 1987; Iyomasa *et al.* 1994; Dantas *et al.* 2003), the acid rocks constitute the basis of the volcanic pile, resting directly over the Botucatu Fm. sandstones. This contact is well exposed in several places along the Paranapanema River valley, locally between the 550 and 450 m topographic levels; up to 100 m variations of the height of this contact correspond, to a large extent, to the dune paleo-landscape of the Botucatu desert, and make it difficult to map and correlate the initial flows. As shown by the geological section A-A´ (Fig. 2), the gentle (1-2°) northward dips of the layers respond for the exposition of this contact at heights above

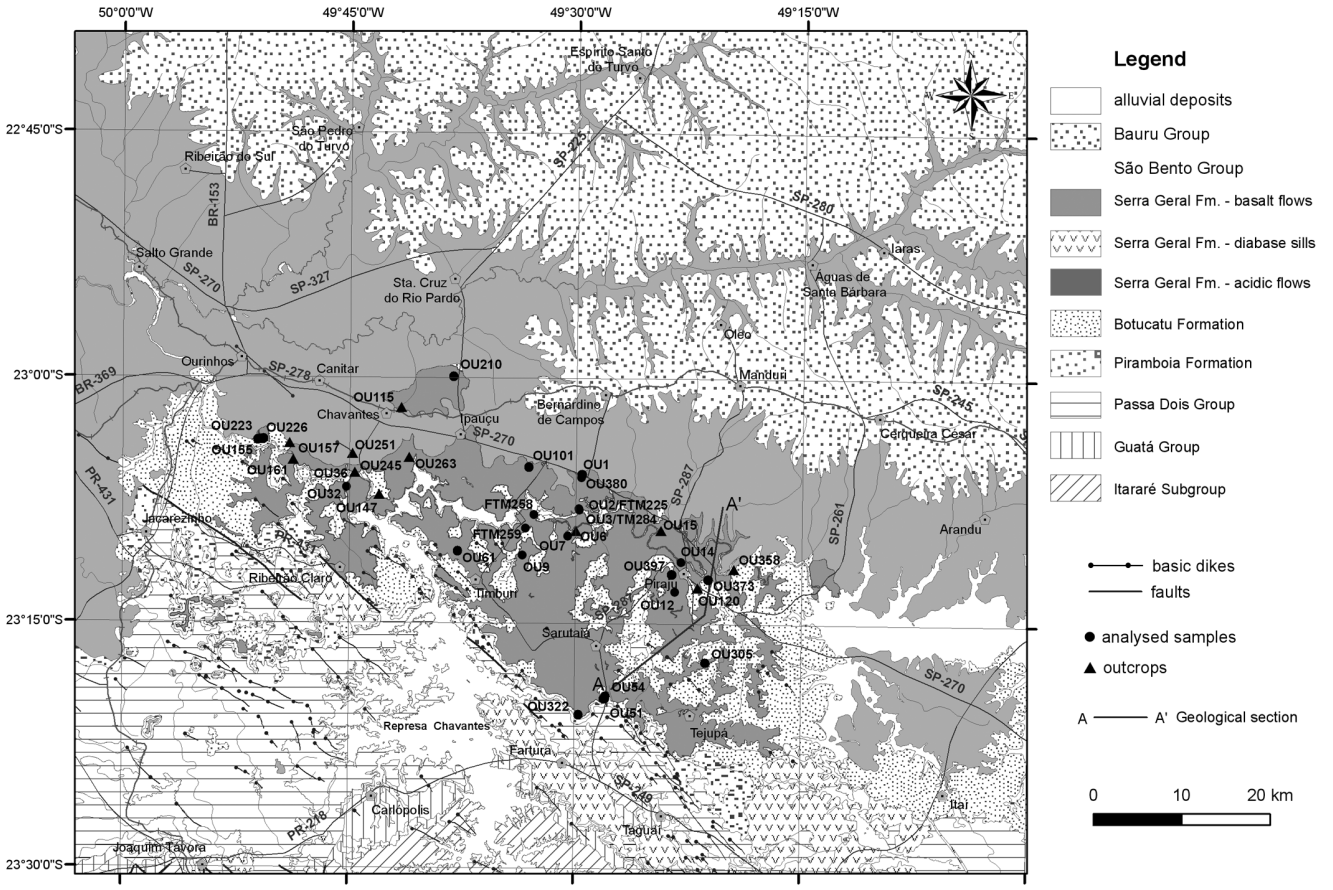

Figure 1 - Geological map of the area of occurrence of acid volcanic rocks in the Piraju-Ourinhos region, with location of samples and outcrops refered to in the text. Simplified from Negri et al. (2006).

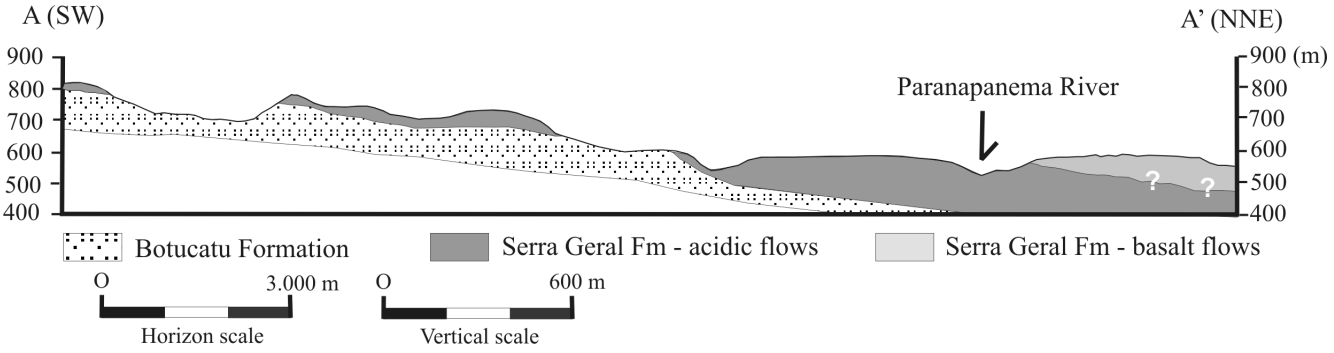

Figure 2 - Geological section from the Serra da Fartura Hill to the Paranapanema River valley.

800 m in the Fartura Hill plateau, *ca.* 15 km south of the Paranapanema River.

Basalt flows cover the acid volcanics, and typically crop out slightly to the north of the Paranapanema River; locally they are covered, in erosive discordance, by sandstones of the Bauru Group (Fig. 1). A small window of acid volcanics exposed by erosion was mapped amid the basalts between the localities of Ipauçu and Chavantes (Fig. 1), but there is no clear evidence that the acid volcanics extend much to the north of this region.

Intrusive subvolcanic bodies, usually of basic composition, are abundant throughout the area, especially intruding the pre-volcanic sediments. Dykes of acid composition are few, but were observed immediately below the lower contact of the flows, in a situation suggestive that they correspond to feeders; the thickest occurrences (over 50 m wide) appear in the Fartura Hill (outcrop OU-54). Diabase dykes with a predominant

N45W direction and variable thickness (some over 100 m) were locally observed cutting dacites (Fig. 3f) and also basalts (cf. Fig. 1; outcrop OU-251); they are however much more abundant cutting the pre-volcanic sediments, and may form swarms (Fig. 1), particularly near the sills. The diabase "sills" are found along discontinuities within or between pre-volcanic sedimentary units, and may form some expressive bodies, such as the Fartura Sill. The occurrence of diabase sills intruding the Botucatu Fm. slightly below the contact with the first dacite flow is a remarkable feature, observed especially in geological sections along the Fartura Hill and in sandstone "windows" exposed amid the dacites (Fig. 1). Some diabase sills appear to intrude the basalt flows; in particular, occurrences of fine to medium-grained diabase are frequent in the lower contact of the basalt pile, and may have crystallized in intrusive bodies (e.g., points OU-157 and OU-358).

Discontinuous levels of inter-flow sandstone, at times with thicknesses over 20 m, constitute an important stratigraphic marker between the acid flows and locally also separate them from the first basalt flow (Fig. 1). The distribution of some bodies of inter-flow sandstone suggests a connection between them and the pre-volcanic sandy substract, a situation that would reflect the filling of interdune valleys by more than one flow.

In the region east of Piraju the acid rocks are covered by thick levels (sometimes over 100 m; cf. Fig. 2) of sandstones that separate them from the overlying basalts (Fig. 1). Although it can be admitted that inter-flow deposits may have reached such thicknesses locally, an alternative explanation is that the acid volcanics would constitute an intrusive body (sill; "lava-dome"); features suggestive of an intrusive contact in a sandstone "roof", as observed in outcrop OU-120, reinforce this interpretation.

The bodies of acid volcanic rock show a well defined zonation (Fig. 4). The central zone, which usually has thicknesses of 10 to 80 m, is made up of gray porphyritic dacite, granular or with "salt and pepper" texture (Fig. 3a); the rock may have a thin subhorizontal layering, given by the alternance of light bands with granular aspect and dark gray bands, which appear to have been originally glassy (Fig. 3c,d). Locally, this thin layering may show asymmetric folding by shearing, associated to flow movements (Fig. 3e).

Towards the upper and lower contacts, the dacite is glassy and typically richer in vesicles, which are only partly filled with fibrous zeolites, calcite and varieties of microcrystalline silica. When in contact with the sandstone, the glassy groundmass changes from dark gray to "chocolate" brown (cf. Fig. 3b), the dacite may be brecciated, and is cut by cm-sized clastic dikes with sandstone infilling (Fig. 3h). In many cases, a significant raise in the magnetic susceptibility is observed: the rock changes from *K* values around 5-10 mSI in the "salt and pepper" or glassy gray dacite to 20-30 mSI in the "chocolate"-brown glassy dacite.

Subhorizontal fracturing, at times very well developed, is characteristic of the central and upper portion of the acid bodies; in levels with "salt and pepper" texture of the upper portion the fracturing changes to subvertical.

PETROGRAPHY The modal classification of the studied acid volcanic rocks is only possible in the few samples with granular texture; the proportion of volcanic glass present in most samples makes it impossible to use modes to name these rocks. As even in the cases of glass-free rocks the very fine-grained texture makes the estimatives imprecise, it was decided to use a chemical classification to name these rocks. The rocks chosen for chemical analysis were those with low proportion of amygdales, or those in which the size of the amygdales allowed the infilling material to be manually extracted during sample preparation. The chemical analyses (see below) show that these acid rocks show a very small compositional variation (65-67 wt% SiO_2; $Na_2O + K_2O$ *ca.* 8 wt%) and plot in the field of trachydacites, very close to the limit with the dacites, in the TAS diagram (Le Bas *et al.* 1986); hence we will refer to these rocks hereafter by the correct name "trachydacites", even if we use "dacite" as the field name.

The trachydacites are always porphyritic, with up to 15 vol.% phenocrysts, mostly plagioclase (up to 5 mm), and subordinately clinopyroxene (augite and pigeonite) and titanomagnetite; the common presence of apatite phenocrysts (Fig. 5c,g) is a remarkable contrast with the associated basalts. The main textural variations reflect changes in crystallinity and grain-size of the groundmass (Figs. 5a to d). When originally glassy, the groundmass usually has microphenocrysts with geometries indicative of quenching, such as feldspar with swallow-tail terminations (Fig. 5e, f) and skeletal opaque minerals. The glass was transformed into a dark-colored microcrystalline aggregate, which consists of altered feldspars and hydrated minerals, and can be compared to palagonite. Less commonly, this groundmass shows relicts of irregular oriented structures whose morphology is suggestive of "fiammées", pointing to the existence of some rocks with pyroclastic features (Fig. 5h). The reddish-brown color of the glassy rocks at the lower contact with the sandstones seems to be associated with the oxidation of the groundmass, which is accompanied, in some samples, by the alteration of the pyroxene phenocrysts.

In some rocks with the macroscopic "salt and pepper" texture it is apparent that the light portions, made up of quartz and feldspars, have round contours, suggesting that they formed from spherulites immerse in glass, which now is transformed into an interstitial turbid mass (Fig. 5c,d).

In the holocrystalline rocks (Fig. 5b), the amygdales are less abundant and phenocrysts are less evident; quartz is always distinguished at the microscope, usually intergrown with the feldspars.

The amygdales, normally 1-20 mm in diameter, may locally reach greater sizes and are filled with zeolites, chalcedony and carbonates.

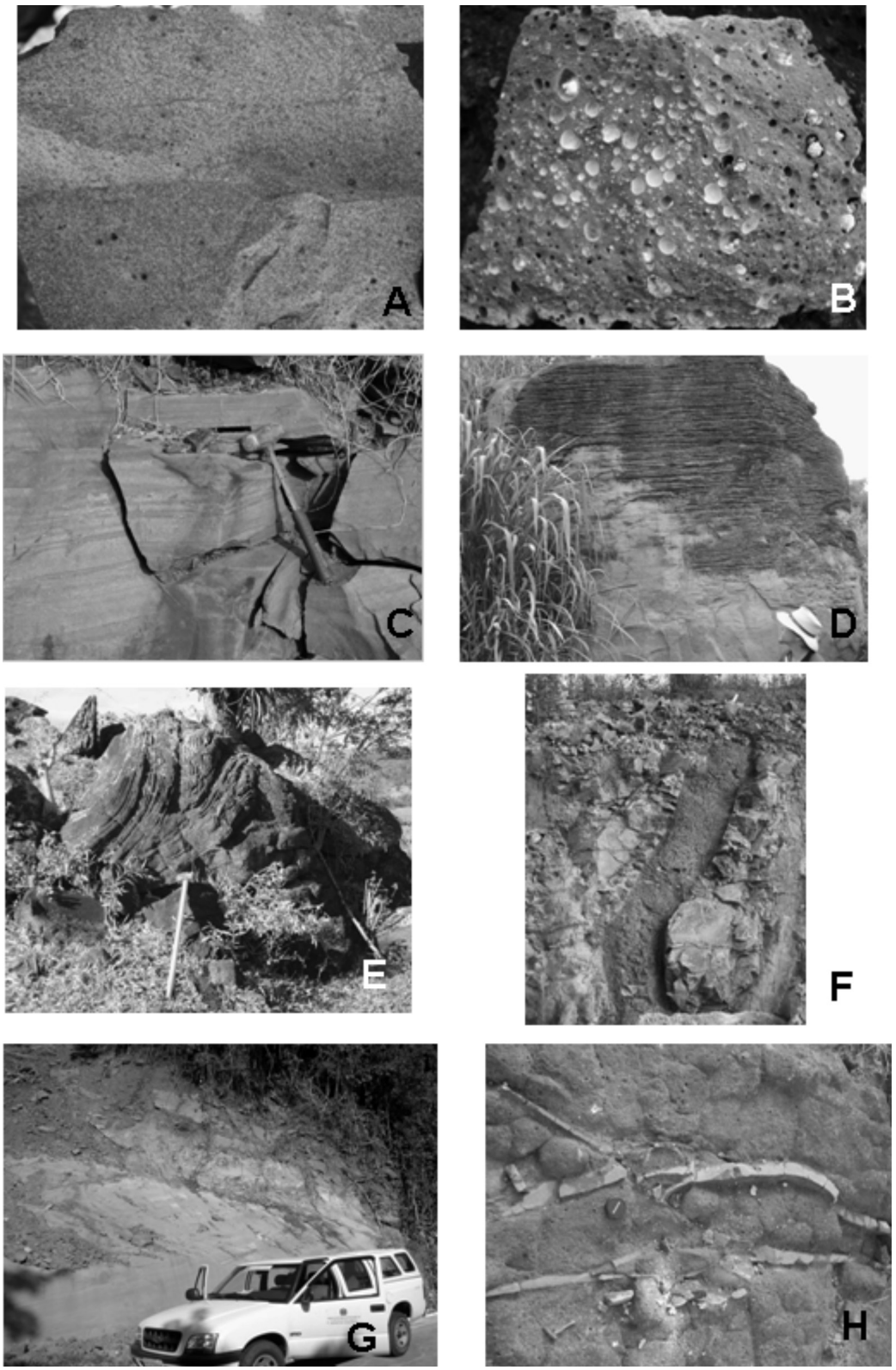

Figure 3 - Field aspects of the acid volcanism in the Piraju-Ourinhos region. (a) macroscopic aspect of the "salt and pepper" texture; (b) glassy amygdaloidal chocolate-brown dacite typical of the upper and lower contacts of the acid volcanic bodies; infilling material is fibrous zeolite; (c, d): aspects of the "rhytmic" layering in vesicle-poor acid volcanic rock; mm-cm-sized light and dark layers seem to derive, respectively, from originally granular and glassy material; (e) asymetric folding of the layering resulting from shearing during lava flow; (f) basalt dyke in acid volcanic rock; (g) lower contact of an acid flow, inclined towards the right side of the image, resting over a Botucatu Fm. Sandstone (at the level of the vehicle); (h) sandstone clastic dykes cutting acid volcanic rock, a feature found next to contacts with underlying sandstones.

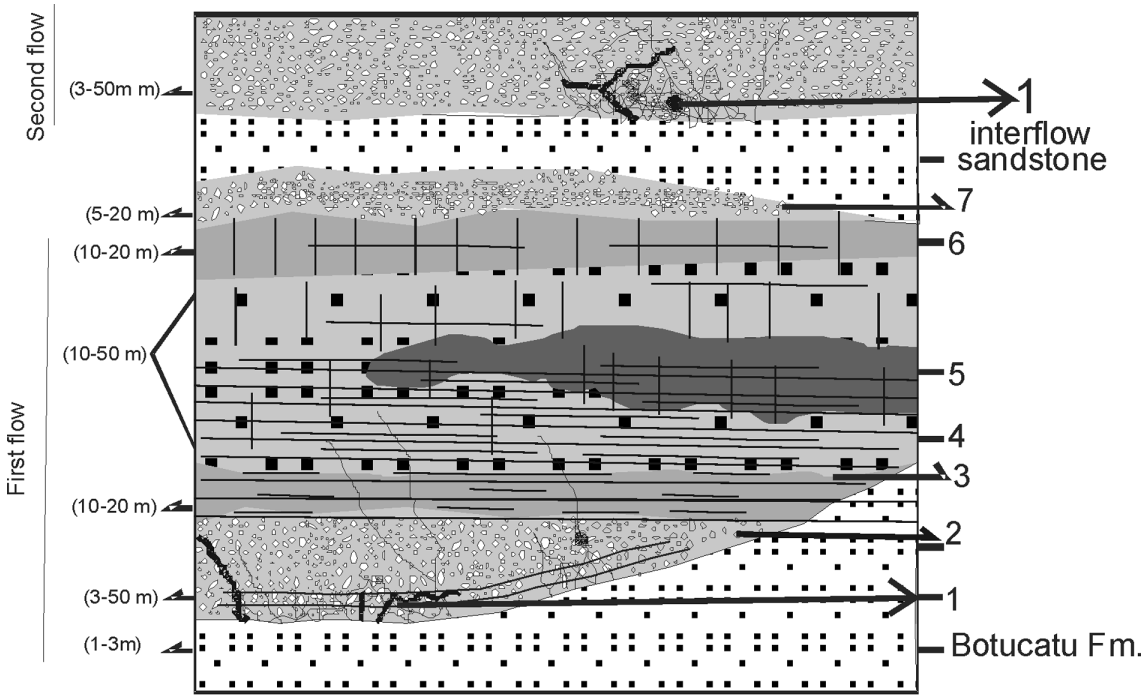

1-Breccia of silicified sandstone and clasts of glassy vesicular chocolate-brown dacite
2-Glassy vesicular/amygdaloidal chocolate-brown dacite
3-Glassy vesicle-poor grey dacite with subhorizontal jointing
4-"Salt and pepper" dacite with subhorizontal jointing passing upwards to columnar jointing
5-Massive granular dacite
6-Glassy grey vesicle-poor dacite with columnar jointing
7-Glassy vesicular/amygdaloidal chocolate-brown dacite

Figure 4 - Sketch geological section of an acid volcanic flow, based in outcrops from the Piraju-Ourinhos region

MINERAL CHEMISTRY Chemical analyses of minerals of the acid volcanic rocks were obtained by electron microprobe following the procedures described by Ruberti (1998), and are presented in tables 1 and 2.

Plagioclase phenocrysts do not show significant core to rim zonation (cf. Table 1, Fig. 6); analyses from different portions of the crystals are typically in the calcic andesine (An_{47-40}) range. In samples with more crystalline groundmass (e.g., OU-07, OU-09), parts of the rims are slightly more sodic, compositionally similar to the microphenocrysts, (An_{36-39}); a subordinate oligoclase rim (An_{20}) was identified in sample OU-07. Alkali feldspar ranges from Or_{57-52} (microphenocrysts in samples OU-14 and OU-02) to albite-rich compositions (Or_{27-14}) in groundmass and rims of swallow-tail plagioclase crystals in sample OU-02 (Table 1; Fig. 6). Even with some uncertainties related to microprobe analyses of very small microphenocrysts and groundmass crystals, the convergence of the two feldspars towards sodic end-members with cooling seems evident.

Two pyroxenes (augite and pigeonite) are present in most of the samples, as scattered phenocrysts and in the groundmass. Crystal zoning is discreet to null, and no significant compositional differences are seen among the different samples. Quadrilateral components (Wo-En-Fs molecules) make up more than 98% of all analyses. Augite compositions mostly concentrate around $Wo_{36}En_{38}Fs_{26}$ (mg#= 62-63). Pigeonite phenocrysts are less abundant, and have average compositions around $Wo_{10}En_{48}Fs_{42}$ (mg#= 55); some microphenocrysts are slightly more iron-rich ($Wo_{11}En_{45}Fs_{44}$; mg#= 50) (Table 2; Fig. 7).

ROCK CHEMISTRY

Analytical procedures and quality control Typical samples of the main textural varieties of acid volcanic rocks were analyzed for whole-rock geochemistry in the laboratories of the Instituto de Geociências, Universidade de São Paulo, in two batches, one by ICP-OES and the other by X-Ray Fluorescence (XRF).

A representative amount of material (typically weighing less than 500 g) was used for geochemical analysis; in rocks bearing amygdales, the infilling material (usually zeolites and silica-group minerals) was manually extracted after the initial crushing of the samples into mm-sized fragments in a hydraulic crusher. The selected fragments were powdered in an agate mill to clay size.

For ICP-OES analyses, 0.25 g sample and 0.75 g flux (lithium meta- + tetraborate) were melted in graphite crucibles at 1000°C for 20 minutes, then dissolved and diluted to a 250 ml 0.2N HNO_3 solution, fol-

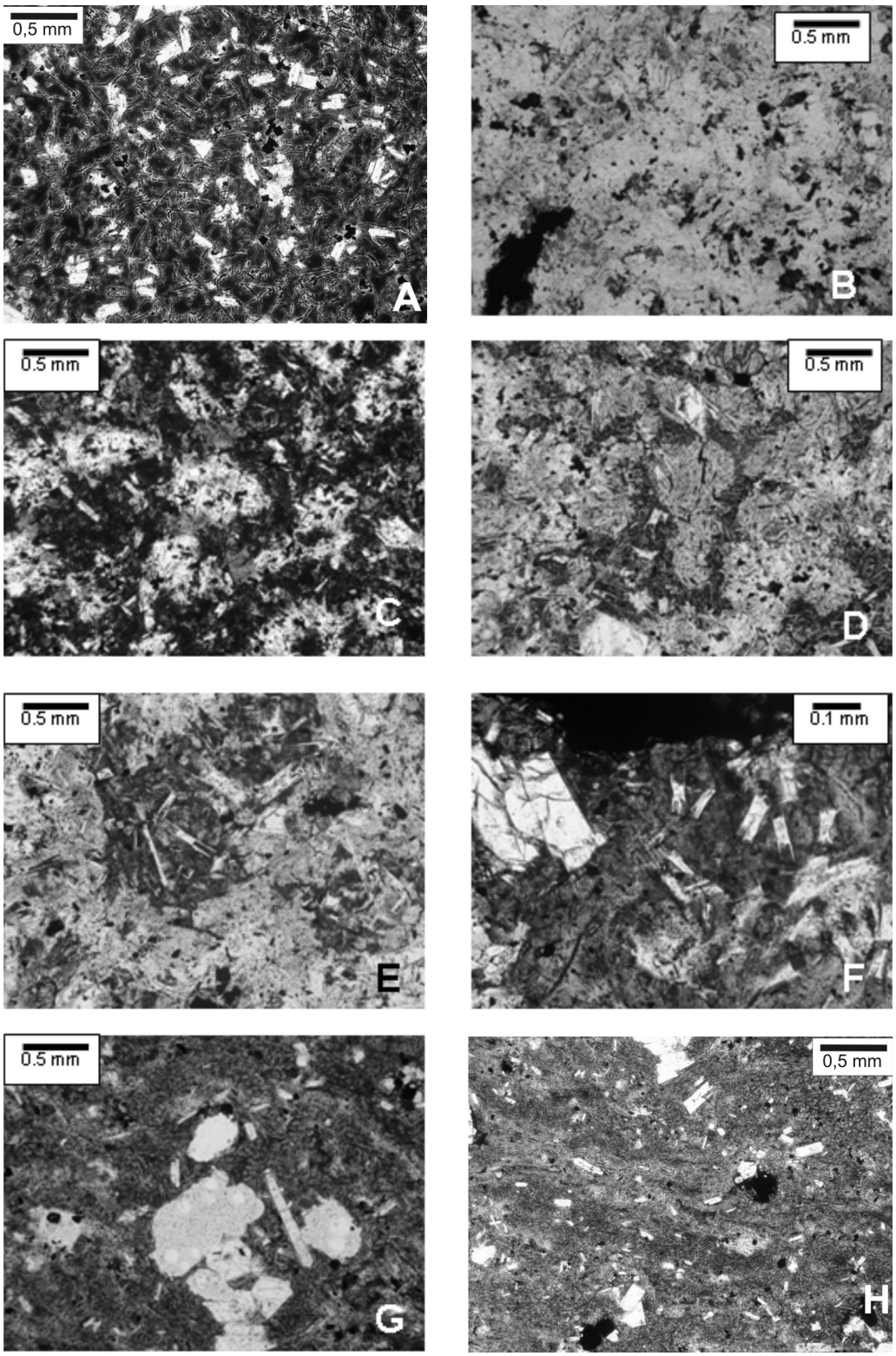

Figure 5 - Textural varieties of the acid volcanic rocks from the Piraju-Ourinhos region. (a) originally glassy texture (dark groundmass, with chocolate-brown color, transformed into a submicroscopic mass, possibly palagonite), with phenocrysts of plagioclase and lesser amounts of clinopyroxene and opaque minerals (sample OU-14); (b) granular texture (sample OU-03a); (c, d) "salt and pepper" texture (light granular portions with sub-rounded shape consisting of alkali feldspar and a SiO_2 mineral surrounded by dark portions of devitrified and hydrated material (respectively, samples TM-284a and OU-15); (e, f) detail of the devitrified dark portions, typically interstitial, showing textures indicative of rapid crystallization, especially plagioclase with "swallow-tail" terminations (respectively, samples OU-36 and TM-225c); (g) plagioclase and apatite phenocrysts in a glassy groundmass (sample OU-06a); (h) groundmass of sample OU-06a, with morphologies suggestive of "fiammées" and therefore of a pyroclastic character. All images in plane-polarized light.

lowing the procedures described by Janasi *et al.* (1995). The XRF analyses of major oxides were obtained from fused glass disks, while a set of trace-elements were analyzed from pressed powder pellets in a Philips PW2100 X-ray Fluorescence Spectrometer at the Instituto de Geociências, Universidade de São Paulo, following the protocol described in Mori *et al.* (1999). The analytical quality for both methods was controlled by analyzing certified international reference materials and duplicates, and the results were considered satisfactory for both major elements (accuracy better than 2% relative for oxides with contents over 10 wt%, and better than 5% for the remaining oxides) and trace-elements (accuracy better than 10% relative when the contents are 10 times greater than detection limit).

A comparison of the results by the two techniques shows that the only systematic difference was in the Zr contents, which are *ca.* 10% lower in the ICP-OES, probably as a reflection of precipitation of this element in the analyzed solution. Comparison with previous analyses for similar rocks in the region show some differences which may be attributed to inter-laboratory differences; chief among them are higher Al_2O_3 and lower MgO in the literature data (Raposo 1987), which are more evident in the basalt dataset (Janasi *et al.* 2007).

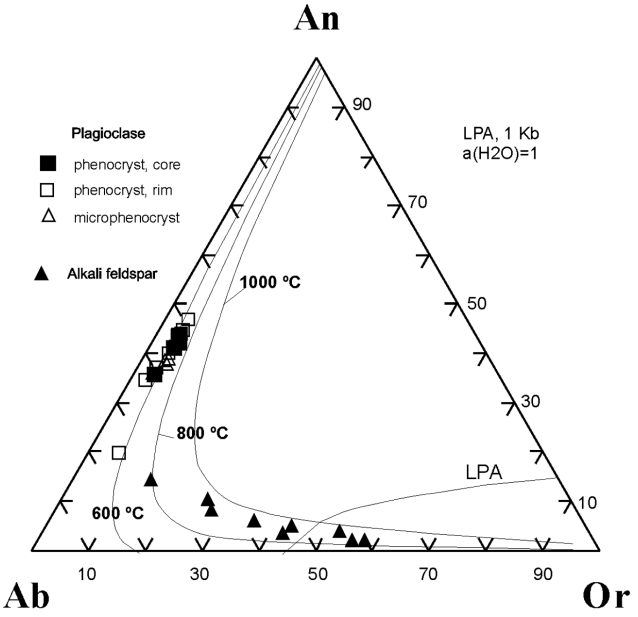

Figure 6 - Composition of feldspars of acid volcanic rocks from the Piraju-Ourinhos region in the Ab-An-Or diagram. The cotectic line (PAL) is from Thompson (1996).

Geochemical variations Although we analyzed acid volcanic rocks from different stratigraphic and geographic positions, representing the main textural varieties observed, the geochemical variations are very small (cf. Table 3), and no chemical criteria to identify distinct flows were identified. The observed dispersion is clearly much smaller than identified in previous works (Raposo 1987, Montanheiro 1999), as shown in figure 8. The smaller dispersion for some elements (Ti, Al, Mg, Fe, P) is to a large extent due to the care taken to extract the vesicle infilling material, as shown by the loss on ignition values which are typically below 1.5 wt% (mostly <1 wt%) in our data, and up to 2.5 wt% in the literature data. The rocks can be characterized as acid (65-67 wt% SiO_2), plotting in the trachydacite field of the TAS diagram (Le Bas *et al.* 1986), ferrous (mg#= 20-27) and metaluminous (A/CNK= 0.85-0.95).

The behavior of some trace-elements in the acid volcanic rocks is shown in Fig. 9, where it is seen that they are characterized by moderate contents of LILE (average 1200 ppm Ba, 330 ppm Sr, 140 ppm Rb), moderate to high Zr (*ca.* 550 ppm Zr from XRF data; as mentioned before, slightly lower values from ICP-OES may be in error), and very low compatible elements (Ni, Cr <10 ppm; V <20 ppm).

The influence of the infilling material over the major-element composition is illustrated by the results for three chocolate-brown glassy samples (Fig. 8). The silica dispersion is related to the type of secondary material filling the vesicles, which is either silica-richer (silica minerals) or poorer (zeolites, calcite) than the rock. Apparently, the concentration of some other oxides in these rocks is not dispersed, but either increased

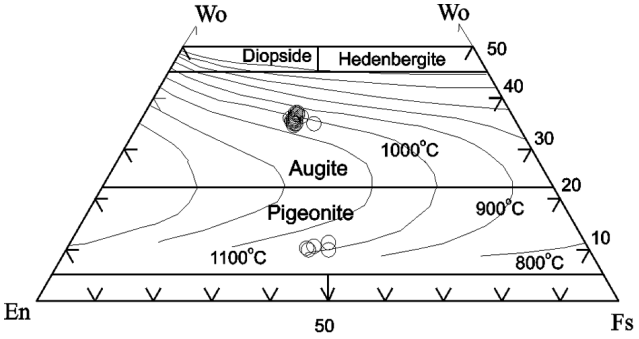

Figure 7 - Compositions of coexisting pyroxenes (augite and pigeonite) in acid volcanic rocks from the Piraju-Ourinhos region in the Wo-En-Fs diagram. Nomenclature after Morimoto (1988); isotherms from the experimental work by Lindsley (1983) at P=1 kbar.

(e.g., Fe, Al) or depleted (Mg, Ca); however, these effects may in part be related to pervasive alteration which changed the color of these particular samples and produced mineralogical effects such as the advanced alteration of the pyroxene phenocrysts. As a result of these transformations, a significant decrease in mg# (down to <5) and increase in A/CNK (to values >1) is observed.

CRYSTALLIZATION TEMPERATURES

Literature shows that the crystallization temperatures of the PEMP acid volcanic rocks are typically very high (≥1000°C), what can explain their non-pyroclastic character (e.g., Bellieni *et al.* 1986; Garland *et al.* 1995). In

Table 1 - Results of chemical analyses of feldspars from trachydacites of the Piraju-Ourinhos region.

Sample	OU-01A	OU-01A	OU-01A	OU-02	OU-02	OU-02	OU-07	OU-07	OU-09	OU-09	OU-09	OU-14	OU-14	OU-14	OU-01A	OU-01A	OU-02	OU-02	OU-02	OU-02	OU-02	OU-14	OU-14
position	mph, c	ph, c	ph, r	ph, r	ph, c	ph, r	ph, c	ph, r	ph, c	ph, r	mph,c	mph, c	ph, c	ph, r	stc, r	stc, r	stc, c	mph	gc	stc, r	stc, c	mph	stc, c
SiO_2	58.54	56.83	57.88	57.71	56.59	58.07	57.10	62.67	58.38	59.19	59.04	58.17	56.47	56.11	65.94	65.14	64.72	67.76	64.95	66.33	64.26	69.71	65.69
TiO_2	0.10	0.06	0.16	0.04	0.08	0.02	0.09	0.16	0.07	0.06	0.07	0.04	0.06	0.04	0.11	0.12	0.09	0.12	0.03	0.39	0.12	0.09	0.13
Al_2O_3	25.16	25.75	25.66	26.15	26.60	26.15	25.43	22.24	24.31	24.50	24.54	25.75	25.44	26.01	19.19	19.23	19.68	17.64	20.37	18.57	21.38	16.41	18.36
FeO(t)	0.62	0.67	0.70	0.67	0.66	0.72	0.62	0.41	0.63	0.49	0.49	0.63	0.73	0.67	0.33	0.33	0.74	0.43	0.58	1.29	0.51	0.81	1.68
MnO	0.01	0.00	0.00	0.00	0.00	0.00	0.00	0.01	0.00	0.02	0.04	0.00	0.00	0.01	0.05	0.01	0.00	0.00	0.00	0.00	0.09	0.00	0.02
MgO	0.04	0.09	0.04	0.06	0.07	0.06	0.07	0.00	0.02	0.01	0.00	0.05	0.08	0.07	0.00	0.00	0.07	0.00	0.03	0.15	0.01	0.09	0.07
CaO	7.68	8.99	8.10	9.32	8.25	8.86	8.28	4.09	7.13	6.99	7.32	7.70	8.82	9.18	1.15	0.94	1.65	0.42	2.02	0.97	2.86	0.38	0.71
Na_2O	6.32	5.90	6.22	5.39	6.09	5.70	6.02	8.52	6.70	6.98	6.76	6.45	5.84	5.75	6.22	5.65	7.03	4.40	6.86	5.51	8.02	3.89	4.49
K_2O	0.70	0.71	0.71	0.69	0.73	0.75	0.76	0.97	0.63	0.46	0.55	0.83	0.78	0.72	5.91	7.19	4.58	8.67	4.21	6.61	2.35	8.40	8.15
Total	99.17	99.00	99.47	100.03	99.07	100.33	98.37	99.07	97.87	98.70	98.81	99.62	98.22	98.56	98.90	98.61	98.56	99.44	99.05	99.82	99.60	99.78	99.30
structural formullae calculated on the basis of 8 oxygens																							
Si	2.644	2.586	2.614	2.593	2.569	2.601	2.608	2.808	2.670	2.679	2.672	2.621	2.591	2.568	2.975	2.964	2.932	3.054	2.919	2.982	2.866	3.117	2.988
Ti	0.003	0.002	0.005	0.001	0.003	0.001	0.003	0.005	0.002	0.002	0.003	0.001	0.002	0.001	0.004	0.004	0.003	0.004	0.001	0.013	0.004	0.003	0.005
Al	1.340	1.382	1.366	1.386	1.424	1.381	1.370	1.175	1.310	1.307	1.309	1.368	1.376	1.403	1.020	1.031	1.051	0.937	1.079	0.984	1.124	0.865	0.985
Fe	0.024	0.026	0.027	0.025	0.025	0.027	0.024	0.015	0.024	0.019	0.019	0.024	0.028	0.026	0.013	0.013	0.028	0.016	0.022	0.049	0.019	0.030	0.064
Mn	0.000	0.000	0.000	0.000	0.000	0.000	0.000	0.000	0.000	0.001	0.002	0.000	0.000	0.000	0.002	0.001	0.000	0.000	0.000	0.000	0.004	0.000	0.001
Mg	0.003	0.006	0.002	0.004	0.005	0.004	0.005	0.000	0.001	0.001	0.000	0.003	0.005	0.005	0.000	0.000	0.005	0.000	0.002	0.010	0.001	0.006	0.005
Ca	0.372	0.438	0.392	0.449	0.401	0.425	0.405	0.196	0.350	0.339	0.355	0.372	0.434	0.450	0.056	0.046	0.080	0.020	0.097	0.047	0.137	0.018	0.035
Na	0.553	0.521	0.544	0.470	0.536	0.495	0.533	0.740	0.594	0.612	0.593	0.563	0.520	0.510	0.545	0.498	0.618	0.384	0.598	0.480	0.694	0.338	0.396
K	0.041	0.041	0.041	0.040	0.042	0.043	0.045	0.055	0.037	0.027	0.032	0.048	0.046	0.042	0.340	0.418	0.265	0.499	0.242	0.379	0.134	0.479	0.473
Total	4.980	5.002	4.991	4.968	5.005	4.976	4.993	4.997	4.988	4.985	4.983	4.999	5.002	5.005	4.954	4.974	4.981	4.915	4.960	4.943	4.982	4.856	4.950
An	38.5	43.8	40.1	46.8	41.0	44.2	41.2	19.8	35.6	34.7	36.2	37.8	43.4	44.9	5.9	4.8	8.3	2.2	10.4	3.6	14.2	2.2	3.8
Ab	57.3	52.1	55.7	49.0	54.7	51.4	54.3	74.6	60.6	62.6	60.5	57.3	52.0	50.9	57.9	51.8	64.2	42.6	63.8	53.9	71.9	40.4	43.8
Or	4.2	4.1	4.2	4.1	4.3	4.4	4.5	5.6	3.8	2.7	3.2	4.9	4.6	4.2	36.2	43.4	27.5	55.2	25.8	42.5	13.9	57.4	52.4

Legend: mph: microphenocryst; ph: phenocrystal; stc: swallow-tail crystal; gc: groundmass crystal; c: core; r: rim; FeO(t): total Fe as Fe^{2+}

this work, we estimated the magma temperatures using different and independent methods, some of which used for the first time in these rocks, as the accessory minerals saturation thermometers.

Coexisting pyroxenes Chemical analyses of coexisting pyroxenes (augite and pigeonite) were obtained by electron microprobe, and used to estimate the crystallization temperature of the magmas by the graphic method of Lindsley (1983), which considers the *solvus* of the Ca-rich and poor clinopyroxenes. The obtained values resulted in temperatures around 1000°C (Fig. 7).

Plagioclase +liquid Estimates of magma temperatures can be obtained from the partition of Ca (or Na) between plagioclase and coexisting liquid.

The estimates obtained in this work considered the liquid composition as that of the whole rock, since no evidence of crystal accumulation is found, whereas the plagioclase composition was obtained by electron microprobe. Estimates of the magma H_2O content (2%) and pressure of crystallization (5-15 kbar) were based in literature data (Garland *et al.* 2005).

The results obtained from the Putirka (2005) calibration are presented in table 3, and show the influence of pressure over the estimated temperature; the val-

Table 2 - Results of chemical analyses of pyroxenes from trachydacites of the Piraju-Ourinhos region.

Sample	OU-01A	OU-01A	OU-01A	OU-01A	OU-02	OU-02	OU-02	OU-02	OU-02	OU-07	OU-07	OU-07	OU-14	OU-14	OU-32	OU-32	OU-32	FTM-259
position	ph, r	ph, c	mph, r	mph, c	ph, r	ph, c	rel, c	mph, r	mph, c	rel, c	ph, r	ph, c	ph, r	ph, c	ph, r	ph, c	mph, c	ph, c
SiO_2	50.06	50.11	50.64	50.38	50.47	50.23	50.63	50.49	51.36	50.47	50.06	50.41	51.06	50.09	50.34	50.44	50.51	49.94
TiO_2	0.54	0.65	0.67	0.69	0.69	0.70	0.58	0.33	0.62	0.43	0.63	0.35	0.69	0.75	0.68	0.66	0.42	0.61
Al_2O_3	1.01	1.25	1.18	1.31	1.30	1.26	1.22	0.64	0.45	0.62	1.20	0.67	1.26	1.40	1.14	1.12	0.66	1.18
FeO(t)	17.54	15.88	15.70	15.42	15.72	15.70	15.93	26.84	24.76	24.71	15.49	24.41	15.22	16.24	15.50	15.42	25.86	15.57
MnO	0.71	0.55	0.64	0.67	0.60	0.62	0.68	1.03	0.99	0.95	0.61	1.06	0.00	0.54	0.58	0.63	1.02	0.60
MgO	11.84	13.21	13.17	13.17	12.97	13.19	13.23	15.51	16.85	16.42	13.08	16.57	13.30	12.64	12.89	12.76	14.97	12.85
CaO	16.59	16.77	17.16	17.07	17.17	16.98	16.71	4.83	4.77	4.78	17.01	4.81	17.53	17.49	17.28	17.63	5.48	17.47
Na_2O	0.20	0.20	0.22	0.20	0.24	0.22	0.23	0.06	0.06	0.07	0.18	0.08	0.24	0.25	0.21	0.26	0.07	0.23
Total	98.49	98.62	99.38	98.91	99.16	98.90	99.21	99.73	99.86	98.45	98.26	98.36	99.30	99.40	98.62	98.92	98.99	98.45
Structural formullae on the basis of 6 oxygens and 4 cations																		
Si	1.949	1.930	1.934	1.934	1.934	1.929	1.938	1.957	1.971	1.965	1.935	1.962	1.948	1.919	1.940	1.938	1.973	1.927
Ti	0.016	0.019	0.019	0.020	0.020	0.020	0.017	0.010	0.018	0.013	0.018	0.010	0.020	0.022	0.020	0.019	0.012	0.018
Al	0.046	0.057	0.053	0.059	0.059	0.057	0.055	0.029	0.020	0.028	0.055	0.031	0.052	0.063	0.052	0.051	0.027	0.054
Fe^{3+}	0.039	0.061	0.055	0.048	0.051	0.061	0.052	0.043	0.007	0.021	0.053	0.032	0.026	0.074	0.044	0.054	0.005	0.073
Fe^{2+}	0.532	0.450	0.446	0.446	0.453	0.443	0.458	0.827	0.787	0.783	0.448	0.763	0.430	0.446	0.456	0.441	0.840	0.430
Mn	0.023	0.018	0.023	0.022	0.019	0.020	0.022	0.034	0.032	0.031	0.020	0.035	0.000	0.018	0.019	0.021	0.034	0.020
Mg	0.687	0.758	0.750	0.754	0.741	0.755	0.755	0.896	0.964	0.953	0.754	0.961	0.756	0.722	0.741	0.731	0.872	0.739
Ca	0.692	0.692	0.702	0.702	0.705	0.699	0.685	0.201	0.196	0.199	0.704	0.201	0.716	0.718	0.714	0.726	0.229	0.722
Na	0.015	0.015	0.016	0.015	0.018	0.016	0.017	0.005	0.004	0.005	0.013	0.006	0.018	0.019	0.016	0.019	0.005	0.017
Wo	35.06	34.95	35.53	35.59	35.80	35.32	34.75	10.03	9.87	10.03	35.59	10.07	36.59	36.30	36.17	36.79	11.59	36.41
En	34.82	38.31	37.94	38.21	37.63	38.17	38.28	44.80	48.52	47.93	38.08	48.28	38.62	36.50	37.54	37.05	44.04	37.27
Fs	30.12	26.74	26.53	26.20	26.57	26.51	26.97	45.18	41.61	42.04	26.33	41.65	24.79	17.20	26.29	26.16	44.38	26.32
mg#	56.4	62.7	62.7	62.8	62.1	63.0	62.2	52.0	55.1	54.9	62.7	55.7	63.7	61.8	61.9	62.4	50.9	63.2

Abbreviations: mph: microphenocryst; ph: phenocryst; rel: relict; c: core; r: rim. mg#= $(Mg/(Mg+Fe^{2+})$

ues obtained at 15 kbar (assuming the plagioclase phenocrysts were formed in magma chambers at the lower crust) are ca. 40°C higher than at 5 kbar. The temperatures at 15 kbar (in the 970-1020°C range) are similar to those obtained by pyroxene geothermometry.

Zircon and apatite saturation Using rock chemistry data, we obtained the saturation temperatures in the accessory minerals zircon and apatite, using the calibrations by Watson & Harrison (1983) and Harrison & Watson (1984), respectively (cf. Table 3).

The chemical dependence of apatite and zircon saturation is different; while apatite is influenced only by the magma SiO_2 contents, zircon saturation depends on the whole rock chemistry, expressed by factor M (Na+K+2*Ca)/(Al*Si); pressure and H_2O do not exert a significant influence in both cases.

The results obtained are represented graphically in figure 10. Average values between 980°C and 1010°C were obtained for apatite saturation; since this mineral occurs as phenocrysts, the temperatures are interpreted as a good estimate of *liquidus*, and are consistent with temperatures obtained by other methods (two pyroxenes and plagioclase-magma geothermometers). Zircon saturation temperatures are significantly lower (on average, 860-890°C), reflecting the Zr undersaturation of these rocks, also evidenced by the absence of this mineral as an early-crystallizing phase– in this respect,

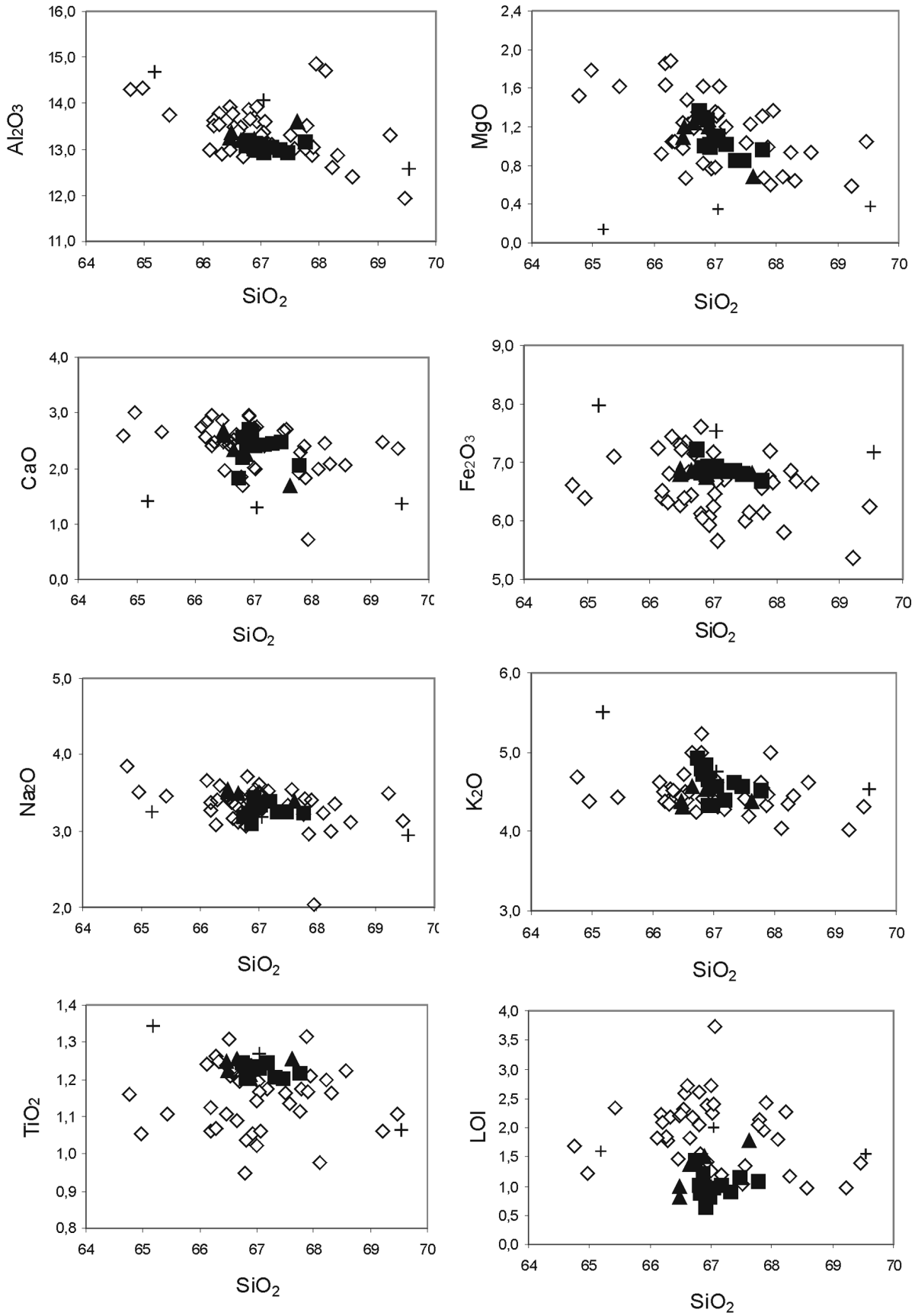

Figure 8 - Variation diagrams for major oxides using SiO_2 as a variation index for acid volcanic rocks from the Piraju-Ourinhos region. Symbols: filled boxes, this work (by XRF); solid triangles, this work (by ICP-OES); crosses, this work (glassy samples without extraction of vesicle-infilling material); open diamonds, previous data (from Raposo 1987).

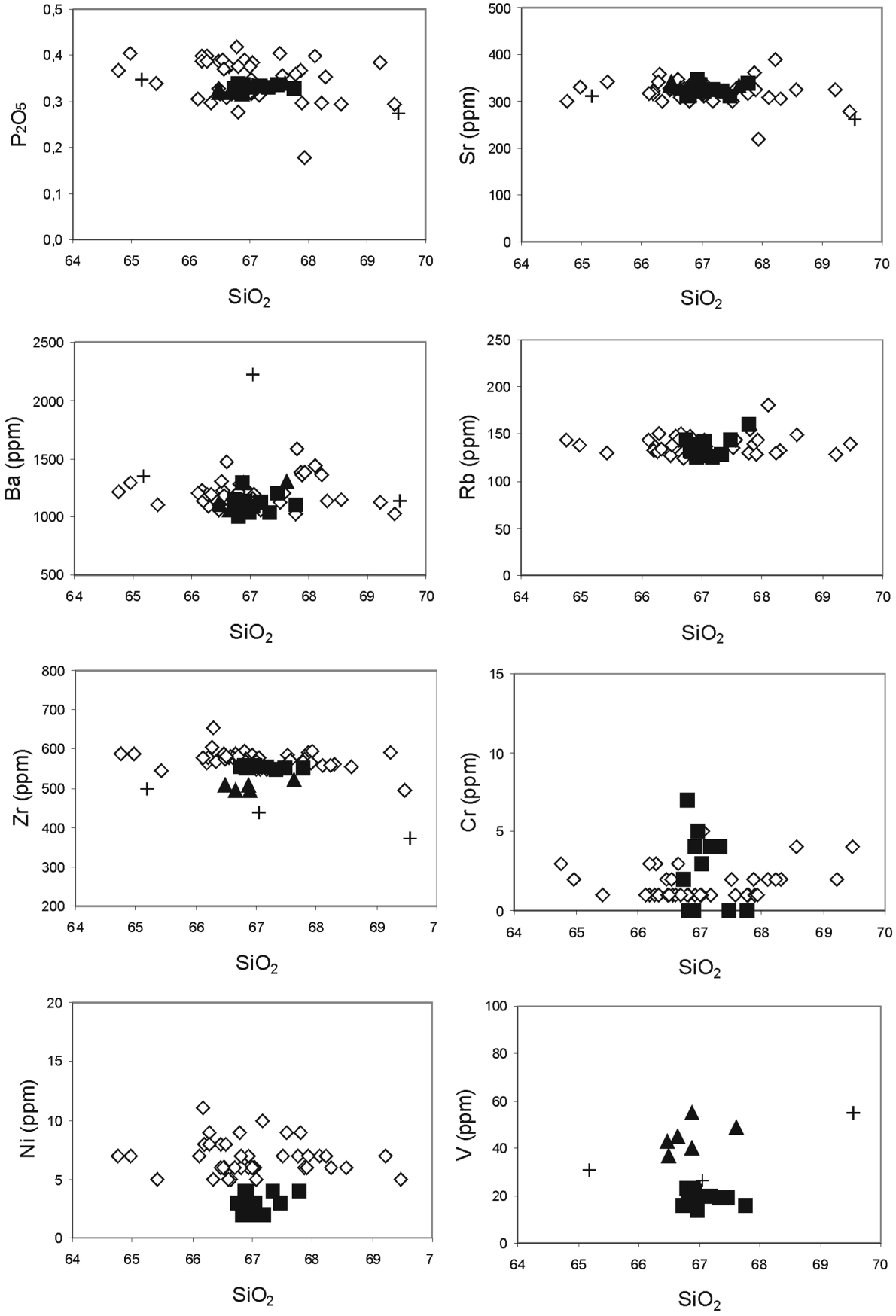

Figure 9 - Variation diagrams for minor and trace-elements using SiO_2 as a variation index for acid volcanic rocks from the Piraju-Ourinhos region. Symbols as in figure 8.

Table 3 - Results of whole-rock chemical analyses of acid volcanic rocks from the Piraju-Ourinhos region.

Sample	OU-51B	OU-54	OU-61	OU-101B	OU-155	OU-210	OU-226B	OU-305A	OU-322	OU-373	OU-380A	OU-397A	OU-01A	OU-02	OU-07	OU-09	OU-12	OU-14a	FTM-225B	FTM-259A	FTM-258
texture	granu-lar	granu-lar	granu-lar	granu-lar	s&p	gg	gg	gg	gg	s & p	s & p	s & p	gg	gg	granu-lar	granu-lar	granu-lar	choc	choc/v	choc/v	choc/v
SiO_2	66.41	65.88	65.88	66.21	65.94	65.59	66.29	65.28	65.66	65.63	66.17	65.22	64.75	64.78	64.94	65.80	65.57	65.05	64.52	63.67	68.17
TiO_2	1.19	1.22	1.21	1.19	1.21	1.21	1.18	1.22	1.18	1.21	1.22	1.21	1.19	1.22	1.22	1.22	1.18	1.18	1.22	1.31	1.04
Al_2O_3	12.90	12.78	12.78	12.77	12.72	12.77	12.71	12.80	12.85	12.89	12.96	12.89	13.03	12.83	12.95	13.24	12.94	12.86	13.54	14.34	12.33
Fe_2O_3t	6.55	6.73	6.83	6.74	6.81	6.71	6.68	7.05	6.79	6.76	6.77	6.67	6.63	6.65	6.73	6.62	6.62	6.62	7.24	7.80	7.02
MnO	0.08	0.10	0.12	0.13	0.13	0.10	0.13	0.09	0.12	0.15	0.13	0.10	0.13	0.10	0.14	0.01	0.12	0.11	0.17	0.17	0.13
MgO	0.94	1.00	1.00	0.84	1.08	1.24	0.84	1.34	0.99	0.97	1.05	1.27	1.17	1.21	1.06	0.67	1.17	1.24	0.33	0.13	0.37
CaO	2.01	2.39	2.67	2.40	2.37	2.36	2.42	1.78	2.53	2.39	2.63	2.15	2.53	2.26	2.62	1.65	2.41	2.19	1.24	1.37	1.34
Na_2O	3.17	3.32	3.38	3.19	3.28	3.03	3.19	3.12	3.18	3.20	3.26	3.11	3.45	3.39	3.43	3.29	3.27	3.28	3.07	3.17	2.89
K_2O	4.42	4.32	4.26	4.55	4.50	4.75	4.48	4.81	4.64	4.57	4.28	4.68	4.20	4.44	4.28	4.26	4.45	4.42	4.57	5.38	4.44
P_2O_5	0.32	0.33	0.32	0.33	0.32	0.32	0.33	0.32	0.32	0.33	0.33	0.33	0.31	0.31	0.32	0.33	0.31	0.31	0.32	0.34	0.27
LOI	1.08	1.02	0.62	0.91	0.97	1.22	1.15	1.43	0.88	0.98	0.80	1.02	0.80	1.36	1.00	1.78	1.20	1.50	2.00	1.59	1.55
Total	99.07	99.09	99.07	99.26	99.33	99.30	99.40	99.24	99.14	99.08	99.60	98.65	98.19	98.55	98.69	98.87	99.24	98.76	98.22	99.28	99.56
Ba	1107	1123	1120	1034	1089	1297	1201	1149	1110	1132	1036	1004	1104	1054	1124	1309	1114	1297	2219	1352	1136
Ce	144	140	154	141	156	148	145	145	129	141	142	115	-	-	-	-	-	-	-	-	-
Co	<2	3	<2	4	<2	4	4	4	<2	4	<2	<2	-	-	-	-	-	-	-	-	-
Cr	<2	4	4	4	3	<2	<2	2	<2	<2	5	7	-	-	-	-	-	-	-	-	-
Cu	14	14	14	12	16	13	16	14	16	15	15	16	-	-	-	-	-	-	-	-	-
F	661	776	775	670	463	656	605	781	835	566	1109	533	-	-	-	-	-	-	-	-	-
Ga	22	22	23	22	22	23	21	23	21	23	21	23	-	-	-	-	-	-	-	-	-
La	59	71	78	76	69	76	65	88	79	67	76	76	74	64	71	66	73	70	58	60	58
Nb	45	46	47	46	47	47	46	48	46	47	47	47	-	-	-	-	-	-			
Nd	73	83	69	67	82	86	85	83	78	79	70	76	-	-	-	-	-	-			
Ni	4	2	4	4	3	4	3	3	2	4	2	3	-	-	-	-	-	-			
Pb	20	26	19	16	18	16	17	15	17	17	17	19	-	-	-	-	-	-			
Rb	160	126	126	129	142	139	144	144	131	134	127	133	-	-	-	-	-	-			
Sc	10	13	12	12	11	14	12	11	10	11	14	12	-	-	-	-	-	-			
Sr	339	326	348	322	322	327	310	314	323	325	335	311	341	327	333	334	325	339	336	311	261
Th	17	20	22	19	20	19	19	19	22	20	21	19	-	-	-	-	-	-			
V	16	20	22	19	20	19	19	16	18	23	14	23	37	45	43	49	55	40	26	31	55
Y	55	62	58	55	60	120	63	78	59	59	58	56	56	57	56	90	55	55	369	63	169
Zn	120	115	106	102	109	108	112	117	110	133	110	108	-	-	-	-	-	-			
Zr	550	555	555	549	555	550	552	555	550	559	558	559	508	495	509	523	509	496	438	497	374
T(Apsat)	999	997	993	999	995	989	1002	987	991	995	999	991	977	977	983	996	986	980	980	976	996
T(Zrsat)	887	877	870	875	875	876	876	886	872	877	876	882	865	864	862	892	868	869	884	888	864
T(Pl-5)	952	958	963	958	957	958	958	945	962	960	964	955	966	959	967	949	962	957	942	952	929
T(Pl-15)	991	998	1004	998	997	998	998	984	1002	1000	1005	995	1006	997	1006	987	1001	996	980	991	966
M	1.64	1.78	1.85	1.78	1.80	1.78	1.78	1.67	1.82	1.77	1.79	1.72	1.81	1.79	1.84	1.53	1.77	1.74	1.41	1.52	1.46

Analyses by XRF (with all trace-elements analysed) and by ICP-OES (only Ba. La. Sr. V. Y and Zr trace-elements analysed)
choc= chocolate-brown trachydacite; /v= with vesicles; gg= glassy gray trachydacite; s & p= salt and pepper.
T(Ap.Zr)sat= apatite and zircon saturation temperatures; T (Pl-5.15)= plagioclase-melt temperature. based in Putirka (2005). at P= 5 and 15 kbar. respectively. All Temperatures in degrees C.
Oxides in wt%; trace-elements in ppm.

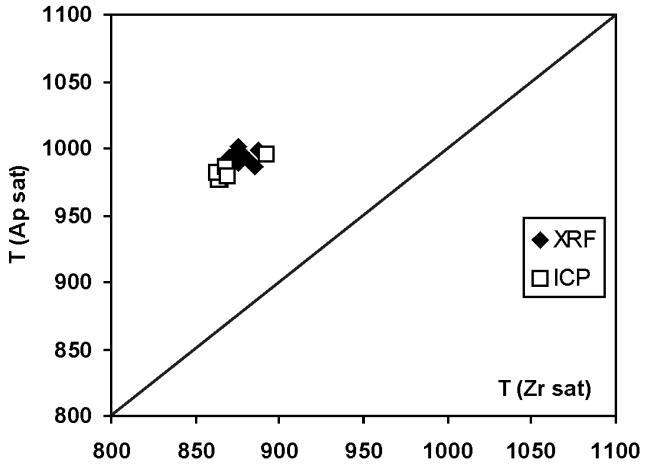

Figure 10 - Zircon and apatite saturation temperatures (in degrees Celsius) for acid volcanic rocks from Piraju-Ourinhos.

it may be mentioned that ongoing electron microscopy studies reveal that baddelleyite is the Zr-bearing phase present in the groundmass of these rocks (V.A. Freitas, Ms Thesis in preparation).

PETROGENETIC ASPECTS The most accepted petrological model for the origin of the parent melts of the Chapecó-type acid volcanic rocks admits that they formed by remelting of high Ti/Y basalt (Bellieni *et al.* 1986; Raposo 1987; Garland *et al.* 1995). The geochemical and isotopic similarities with the geographically associated high Ti/Y basalts clearly suggest a genetic link with the basic magmatism, and the absence of intermediate compositions is an argument against derivation by crystal fractionation. Garland *et al.* (1995), however, admitted an alternative model in which a compositional gap (defined by a rapid raise in the silica content) could be generated during crystal fractionation if an expressive increase in the proportion of magnetic in the solid extract occurs. On the other hand, in the Piraju region the initial $^{87}Sr/^{86}Sr$ of the trachydacites are slightly higher than those of the associated basalts (ca. 0.708 x 0.706; Raposo 1987), requiring the participation of additional higher time-integrated Rb/Sr sources in their generation.

The hypothesis of remelting of basalt underplates has been considered to explain satisfactorily the generation of magmas equivalent to the Chapecó-type trachydacites from trace-element geochemical modeling (Raposo 1987; Garland *et al.* 1995). These modelings are based in the behavior of incompatible elements, and suggest relatively low partial melting rates (ca. 20-30%), which are required to promote the observed enrichments. Modeling of equilibrium fractional melting using compatible-incompatible element pairs (Freitas *et al.* 2006) suggests some additional constraints to this model, since the contents of compatible elements such as Ni and V in the trachydacites are significantly lower than predicted from melting typical high-Ti basalts (or their high-pressure equivalents); it seems necessary, to reach these contents, that the magmas have been subject to some fractionation. On the other hand, the Zr-undersaturated character of the Piraju-Ourinhos acid rocks is not consistent with their derivation by crystal fractionation involving zircon from Chapecó-type magmas equivalent to those from the Guarapuava region, as suggested by Garland *et al.* (1995) and Peate (1997). More probably, Zr undersaturation reflects a feature of the sources of the parent magmas of these trachydacites.

The above considerations suggest that the hypotheses for the generation of acid magmatism in the PEMP must be subject to additional refinements, which could be particularly successful with the use of modern chemical and isotope analyses in samples for which there is detailed field and petrographic control.

Acknowledgements This work was financed by a Grant by FAPESP to TJM (Proc. 03/06259-4). FAD and PMS aknowledge CNPq and VAF FAPESP for the granting of Scientific Initiation Scholarships; VAJ thanks CNPq for a Scientific Productivity Scholarship. We acknowledge a careful review by an annonymous referee which helped improve the final version of this article.

References

Bellieni G., Brotzu P., Comin-Chiaramonti P., Ernesto M., Melfi A., Pacca I.G., Piccirillo E.M. 1984. Flood basalt to rhyolite suites in the southern Parana Plateau (Brazil): palaeomagnetism, petrogenesis and geodynamic implications. *Journal of Petrology*, **25**:579-618.

Bellieni G., Comin-Chiaramonti P., Marques L.S., Melfi A.J., Nardy A.J.R., Papatrechas C., Piccirillo E.M., Roisenberg A., Stolfa D. 1986. Petrogenetic aspects of acid and basaltic lavas from the Paraná plateau (Brazil): geological, mineralogical and petrochemical relationships. *Journal of Petrology*, **27**:915-944.

Dantas F.A., Janasi V.A., Ruberti E. 2003. Rochas vulcânicas ácidas cretáceas da Bacia do Paraná, região de Piraju-Ourinhos (SP): petrografia, química mineral e química de rochas. *In*: SBG, Simpósio de Geologia do Sudeste, 8, São Pedro (SP), *Boletim de Resumos*, p. 70.

Ernesto M., Raposo M.I., Marques L.S., Renne P.R., Diogo L.A., de Min A. 1999. Paleomagnetism, geochemistry and ^{40}Ar-^{39}Ar dating of the North-eastern Paraná Magmatic Province: tectonic implications. *Journal of Geodynamics*, **28**:321-340.

Freitas V.A, Janasi V.A., Montanheiro T.J., Reis P.M. 2006. Gênese e evolução das rochas vulcânicas ácidas da Província Magmática Paraná na região de Piraju-Ourinhos (SP) a partir de dados geoquímicos de minerais e rochas. *In*: SBG, Congresso Brasileiro de Geologia, **43**, Aracaju,

Boletim de Resumos, p. 256.

Garland F., Hawkesworth C.J., Mantovani M.S.M. 1995. Description and petrogenesis of the Paraná rhyolites, southern Brazil. *Journal of Petrology*, **36**:1193-1227.

Harris C., Milner S. 1997. Crustal origin for the Paraná rhyolites: Discussion of Description and Petrogenesis of the Paraná Rhyolites, Southern Brazil' by Garland *et al.* (1995). *Journal of Petrology*, **38**:299-302.

Harrison T.M. & Watson E.B. 1984. The behavior of apatite during crustal anatexis: Equilibrium and kinetic considerations. *Geochimica et Cosmochimica Acta*, **48**:1468-1477.

Iyomasa W.S., Fernandes L.A., Frascá M.H.B.O., Scarmínio M. 1994. As rochas vulcânicas ácidas da Formação Serra Geral no vale do Rio Paranapanema (SP/PR). *In*: SBG, Congresso Brasileiro de Geologia, 38, Balneário de Camboriú/SC, *Boletim de Resumos*, p. 107-108.

Janasi V.A., Negri F.A., Montanheiro T.J., Freitas V.A.; Rocha B.C., Reis P.M. 2007. Geochemistry of the eocretacic basalt magmatism in the Piraju-Ourinhos region, SE Brazil, and implications to the stratigraphy of the Serra Geral Formation. *Revista Brasileira de Geociências*, **37**:148-162.

Janasi V.A., Andrade S., Ulbrich H.H.G.J. 1995. A correção do drift instrumental em ICP-AES com espectrômetro seqüencial e a análise de elementos maiores, menores e traços em rochas. *Boletim IG-USP*, *Série Científica*, **26**:45-58.

Le Bas M.J., Le Maitre T.W., Streckeisen A., Zanettin B. 1986. A chemical classification of volcanic rocks based on the total alkali-silica diagram. *Journal of Petrology*, **27**:745-750.

Lindsley D. 1983. Pyroxene thermometry. *American Mineralogist*, **68**:477-493.

Montanheiro T.J. 1999. *Prospecção e caracterização de pozolanas na Bacia do Paraná, Estado de São Paulo*. Tese de Doutoramento, Instituto de Geociências, Universidade de São Paulo, 226p.

Mori P.E., Reeves S., Correia C.T., Haukka M. 1999. Development of a fused glass disc XRF facility and comparison with the pressed powder pellet technique at Instituto de Geociências, São Paulo University. *Revista Brasileira de Geociências*, **29**(3):441-446.

Morimoto N. 1988. Nomenclature of pyroxenes. *Mineralogy and Petrology*, **39**:55-76.

Negri F.A., Montanheiro T.J., Janasi V.A., Reis P.M. 2006. Mapa de distribuição das rochas vulcânicas nas folhas Piraju/SP e Jacarezinho/SP-PR. *In*: SBG, Congresso Brasileiro de Geologia, 43, Aracaju, *Boletim de Resumos,* p. 247.

Peate D. 1997. The Paraná-Etendeka Province. *In*: Mahoney J.J., Coffin M.F. (eds.) *Large Igneous Provinces*. Geophysical Monograph **100**, AGU, p. 217-245.

Putirka K.D. 2005. Igneous thermometers and barometers based on plagioclase + liquid equilibria: Tests of some existing models and new calibrations. *American Mineralogist*, **90**:336-346.

Raposo M.I. 1987. *Evolução magmática e petrológica das rochas vulcânicas ácidas mesozóicas da região de Piraju-Ourinhos (SP e PR)*. Dissertação de Mestrado, Instituto Astronômico e Geofísico, Universidade de São Paulo, 159 p.

Ruberti E. 1998. *Petrologia e geoquímica das suítes carbonatíticas de Mato Preto (PR) e da Barra de Itapirapuã (PR-SP)*. Tese de Livre-Docência, Instituto de Geociências, Universidade de São Paulo, 211 p.

Stewart K., Turner S., Kelley S., Hawkesworth C., Kirstein L., Mantovani M. 1996. 3-D, ^{40}Ar-^{39}Ar geochronology in the Paraná continental flood basalt province. *Earth and Planetary Science Letters*, **143**:95-109.

Thompson A.B. 1996. Fertility of crustal rocks during anatexis. *Transactions of the Royal Society of Edinburgh: Earth Sciences*, **87**:1-10.

Watson E. B. & Harrison T. M. 1983. Zircon saturation revisited: temperature and composition effects in a variety of crustal magma types. *Earth and Planetary Science Letters*, **64**:295-304.

Manuscrito ID 7812
Submetido em 27 de abril de 2007
Aceito em 01 de dezembro de 2007
Sistema eletrônico de submissão